

Optical Hanle effect in fields of arbitrary strength and bandwidth

P. Anantha Lakshmi and G. S. Agarwal

School of Physics, University of Hyderabad, Hyderabad-500 001, India

(Received 21 March 1980)

A quantum-statistical theory of optical Hanle effect is developed for arbitrary intensities and bandwidths of the pump field. The excited- and ground-state level shifts, caused by another light field with appropriate polarization, are directly included in the theory by using the method of time averaging. The laser fluctuations are taken into account exactly by using the phase-diffusion model of the pump laser. The analytical and numerical results for the fluorescence signals are presented for a variety of excitations. Our results in the limiting case reduce to those of Kaftandjian, Klein, and Hanle. Finally, the case of a very broadband excitation under saturation conditions is analyzed and the results for signals in various directions and the polarizations are obtained.

I. INTRODUCTION

The Hanle effect has been extensively used in the study of the lifetimes of the excited states and the measurement of various relaxation and collision parameters.¹⁻⁹ In the normal Hanle effect, one studies the properties of the magnetic sublevels by preparing the system in a coherent superposition of the Zeeman sublevels and by observing the fluorescence from such a coherent superposition as a function of the magnetic field. The coherent superposition^{5,10,11} can be achieved either by using a broadband source or by using a monochromatic pump. The linewidth of the observed signal has been seen to be critically dependent on the nature of the exciting source.^{5,10} Several variations¹²⁻¹⁷ of the Hanle effect have been proposed and used in the high-resolution work. For instance, it has been shown that a modulated pump field leads to fluorescence variation that immediately yields not only the relaxation parameters but also the excited-state splittings.¹²⁻¹⁴ A novel variation^{15,16} of the Hanle experiment involves the use of a suitably polarized radiation to lift the degeneracy of the excited states, i. e., each energy level is shifted by a different amount due to light shifts.¹⁸⁻²⁰ Thus the properties of the magnetic sublevels could be studied by using another strong off-resonance laser, in addition to the pump laser, whose frequency and intensity could be easily varied.¹⁵⁻¹⁷ The fluorescence is now observed as a function of the intensity or the frequency of the strong off-resonant laser field. In this case it has been found by Kaftandjian *et al.*¹⁵ that the zero-field level crossings occur in the same manner as in the normal Hanle effect (using the magnetic fields).

In this paper we develop a general theory of the optical Hanle effect. The theory is valid for arbitrary values of the strength and bandwidth of the pump field. In the limiting case of a weak monochromatic pump, our results go over to the standard results. Our theory is also applicable to

cases when a broadband source is used in place of the monochromatic pump. For simplicity, we restrict our considerations only to the case when the levels involved in the Hanle transitions correspond to the levels with total angular momentum $J=0$ and 1, respectively. In Sec. II we present the general formulation and show how the bandwidth effects²¹ of the pump field could be included in the equations of motion of the density matrix. We also show how the off-resonant strong field leads to the light-shift terms in the equations of motion. Such equations are solved in the steady state in Sec. III, and we present expressions for the fluorescence signals in different directions. A number of special cases of our results are also discussed in Sec. III. Finally, we present a numerical study of the fluorescence signals and discuss how the signals change by varying the strength and the bandwidth of the exciting laser. In Sec. IV optical Hanle effect in intense broadband fields is treated rigorously.

II. DENSITY MATRIX FORMULATION OF OPTICAL HANLE EFFECT

In this section we present the density matrix formulation of the optical Hanle effect. We obtain the most general equations valid for arbitrary values of the field strengths and arbitrary values of its bandwidth. For simplicity and in view of the recent experimental work¹⁷ on optical Hanle effect, we restrict our considerations only to the case when the two levels involved in the transition possess angular momenta 0 and 1, respectively. The energy-level diagram is schematically shown in Fig. 1.

The geometry used in optical Hanle effect is shown in Fig. 2. The physical situation in optical Hanle effect corresponds to a circularly polarized light propagating along the z axis intersecting the atomic beam directed along the x axis. A second linearly polarized laser beam (which will hereafter

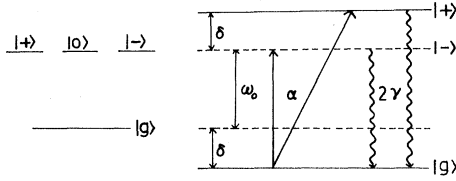


FIG. 1. Schematic representation of the energy levels involved in optical Hanle effect.

be referred to as the pump) propagating along the z axis, with its electric vector making an angle θ with the x direction, interacts with the laser beam. The linearly polarized light creates the atomic coherences, i. e., it prepares the atomic system in a coherent superposition of the excited states. The atomic coherences are monitored by observing the fluorescence signals in different directions. Two common situations used for observing fluorescence correspond to the detection of the radiation in the directions (i) x with polarization along the y axis, (ii) y with its polarization along the x axis. The circularly polarized off-resonant radiation lifts the degeneracy of the excited states and also shifts the ground state. The role of the circularly polarized radiation is similar to the role of the magnetic field used in the usual Hanle experiments, with the difference that the magnetic field does not shift the ground state. It is well known that when a two-level atom is subjected to an off-resonant light field, its ground and excited states are shifted by equal amounts, but in opposite directions.¹⁸ The magnitude of the light shift is β^2/Δ_c , where β is the Rabi frequency of the transition and Δ_c is the difference between the frequency of the atom and the light field. For our system, we expect that the levels $|+\rangle$ (corresponding to the magnetic quantum number $+1$) and $|g\rangle$ will be shifted in opposite directions if the circularly polarized light is left-handed; this will be shown explicitly later. In Fig. 1 the positions of the shifted levels are shown.

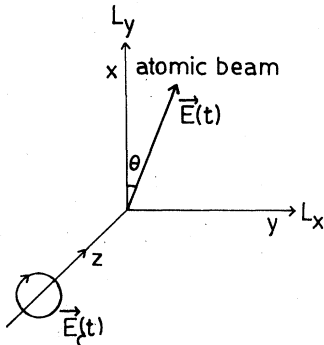


FIG. 2. Schematic diagram showing the directions and polarizations of the various beams.

The total Hamiltonian for the system interacting with the pump field $\vec{E}(t)$ and the circularly polarized field $\vec{E}_c(t)$ can be written as:

$$H = \hbar\omega_0(A_{++} + A_{--}) - [\vec{d}_{+g} \cdot \vec{E}(t)A_{+g} + \vec{d}_{-g} \cdot \vec{E}(t)A_{-g} + \text{H. c.}] - [\vec{d}_{+g} \cdot \vec{E}_c(t)A_{+g} + \text{H. c.}], \quad (2.1)$$

where A_{ij} are the operators $|i\rangle\langle j|$, \vec{d}_{ij} are the dipole-moment matrix elements, and $\omega_0 = (E_+ - E_g)/\hbar$. The pump field is written in the form

$$\vec{E}(t) = \mathcal{E}_0(t)(\hat{x}\cos\theta + \hat{y}\sin\theta)e^{-i\omega_L t + i\varphi(t)} + \text{c. c.} = \vec{\mathcal{E}}(t)e^{-i\omega_L t} + \text{c. c.}, \quad (2.2)$$

where, as shown in Fig. 2, the angle θ gives the direction of polarization of the pump. The functions $\mathcal{E}_0(t)$ and $\varphi(t)$ are taken to be slowly varying functions of time. For a strictly monochromatic field $\mathcal{E}_0(t)$ and $\varphi(t)$ are independent of time t and are *not* random variables. For a fluctuating field, $\mathcal{E}_0(t)$ and $\varphi(t)$ are stochastic functions. The frequency of the pump is either at resonance or close to resonance with the frequency of the $J=0$ to $J=1$ transition. The terms in the last brackets in (2.1) represent the interaction of the system with the circularly polarized radiation

$$\vec{E}_c(t) = \vec{\mathcal{E}}_c e^{-i\omega_c t} + \vec{\mathcal{E}}_c^* e^{i\omega_c t}. \quad (2.3)$$

The density matrix ρ of the system satisfies the equation

$$\frac{\partial \rho}{\partial t} = \frac{-i}{\hbar} [H, \rho] + L_{\text{inc}} \rho, \quad (2.4)$$

where the effect of spontaneous emission, as well as that of the decay mechanisms and pumping process, is contained in L_{inc} , which has the structure²²

$$(L_{\text{inc}}\rho)_{ij} = \delta_{ij} \sum_{k \neq i} 2\gamma_{ik} \rho_{kk} - \left(\sum_{k \neq i} \gamma_{ki} + \sum_{k \neq j} \gamma_{kj} \right) \rho_{ij}, \quad (2.5)$$

where $2\gamma_{ij}$ represents the transition probability per unit time, from the level j to the level i , due to spontaneous, collisional and all other incoherent processes. On transforming (2.4) to a frame rotating with the angular frequency of the pump field ω_L , and on making a rotating wave approximation, (2.4) reduces to

$$\frac{\partial \rho^{(R)}}{\partial t} = \frac{-i}{\hbar} [H^{(R)}(t), \rho^{(R)}] + L_{\text{inc}} \rho^{(R)} - i[GA_{+g} e^{i(\omega_L - \omega_0)t} + G^* A_{g+} e^{-i(\omega_L - \omega_0)t}, \rho^{(R)}], \quad (2.6)$$

where all the slow time dependence is contained in $H^{(R)}(t)$ and the fast time dependence in the $\rho^{(R)}$

equation is explicitly displayed. $H^{(R)}(t)$ and G are given by

$$H^{(R)}(t) = [-\vec{d}_{+g} \cdot \vec{\mathcal{E}}(t) A_{+g} - \vec{d}_{-g} \cdot \vec{\mathcal{E}}(t) A_{-g} + \text{H. c.}] + \hbar(\omega_0 - \omega_L)(A_{++} + A_{--}), \quad (2.7)$$

$$G = (\vec{d}_{+g} \cdot \vec{\mathcal{E}}_c / \hbar). \quad (2.8)$$

The matrix elements of $\rho^{(R)}$ are related to ρ by

$$\rho_{ij}^{(R)}(t) = \delta_{ij} \rho_{ij}(t) + (1 - \delta_{ij}) \rho_{ij}(t) e^{i\omega_{ij}(t)}, \quad (2.9)$$

$$\omega_{+g} = \omega_{-g} = \omega_L, \quad \omega_{+-} = 0.$$

As a first step in the calculation we show how the rapidly oscillating terms in (2.6) lead to light shifts. For this purpose, we use Bogoliubov-Mitropolsky's method of time averaging. This method when applied to the density matrix equation^{23,24}

$$\partial \rho / \partial t = L_0 \rho + L_1(t) \rho \quad (2.10)$$

shows that the effect of rapidly oscillating terms in $L_1(t)$ in leading order could be taken into account by replacing (2.10) by

$$\frac{\partial \rho}{\partial t} = L_0 \rho + L_1(t) \int_{-\infty}^t L_1(\tau) \rho(t) d\tau. \quad (2.11)$$

On using (2.11), we find that (2.6) reduces to

$$\frac{\partial \rho^{(R)}}{\partial t} = \frac{-i}{\hbar} [H'(t), \rho^{(R)}] + L_{\text{inc}} \rho^{(R)}, \quad (2.12)$$

where

$$H'(t) = -[\vec{d}_{+g} \cdot \vec{\mathcal{E}}(t) A_{+g} + \vec{d}_{-g} \cdot \vec{\mathcal{E}}(t) A_{-g} + \text{H. c.}] + \hbar(\omega_0 - \omega_L + \delta) A_{++} + \hbar(\omega_0 - \omega_L) A_{--} - \delta A_{gg}, \quad (2.13)$$

where

$$\delta = |G|^2 / (\omega_L - \omega_c). \quad (2.14)$$

The effective Hamiltonian (2.13) now explicitly has light shift terms $\delta(A_{++} - A_{gg})$.

We next eliminate the explicit θ dependence and the phase dependence from the Hamiltonian by making use of the relations among the dipole matrix elements

$$\vec{d}_{+g} = R(-\hat{x} + i\hat{y}), \quad \vec{d}_{-g} = R(\hat{x} + i\hat{y}) \quad (2.15)$$

and by making the transformations

$$\begin{aligned} \tilde{\rho}_{ii} &= \rho_{ii}, \quad \tilde{\rho}_{+-} = -\rho_{+-} e^{2i\theta}, \\ \tilde{\rho}_{+g} &= -\rho_{+g} \exp[i(\theta + \varphi(t) + \omega_L t)], \\ \tilde{\rho}_{-g} &= \rho_{-g} \exp[i(\varphi(t) - \theta + \omega_L t)]. \end{aligned} \quad (2.16)$$

We further assume only the radiative decay from the level $| \pm \rangle$ to the ground level $| g \rangle$ at the rate 2γ and include no other decays. In such a case, the density matrix elements $\tilde{\rho}_{ij}$ satisfy the equations

$$\begin{aligned} \dot{\tilde{\rho}}_{++} &= i\alpha \tilde{\rho}_{g+} - i\alpha^* \tilde{\rho}_{+g} - 2\gamma \tilde{\rho}_{++}, \\ \dot{\tilde{\rho}}_{--} &= i\alpha \tilde{\rho}_{g-} - i\alpha^* \tilde{\rho}_{-g} - 2\gamma \tilde{\rho}_{--}, \\ \dot{\tilde{\rho}}_{gg} &= -i\alpha(\tilde{\rho}_{g+} + \tilde{\rho}_{g-}) + i\alpha^*(\tilde{\rho}_{+g} + \tilde{\rho}_{-g}) \\ &\quad + 2\gamma(\tilde{\rho}_{++} + \tilde{\rho}_{--}), \\ \dot{\tilde{\rho}}_{+-} &= -(2\gamma + i\delta)\tilde{\rho}_{+-} + i\alpha \tilde{\rho}_{g-} - i\alpha^* \tilde{\rho}_{+g}, \\ \dot{\tilde{\rho}}_{+g} &= -[2i\delta + \gamma + i\mu(t)]\tilde{\rho}_{+g} + i\alpha(\tilde{\rho}_{gg} - \tilde{\rho}_{+-} - \tilde{\rho}_{-+}), \\ \dot{\tilde{\rho}}_{-g} &= -[i\delta + \gamma + i\mu(t)]\tilde{\rho}_{-g} + i\alpha(\tilde{\rho}_{gg} - \tilde{\rho}_{+-} - \tilde{\rho}_{-+}), \end{aligned} \quad (2.17)$$

where

$$\dot{\varphi}(t) = \mu(t) \quad \text{and} \quad \alpha = R\mathcal{E}_0(t). \quad (2.18)$$

The above equations could be solved if $\mu(t)$ and $\mathcal{E}_0(t)$ were constants, as in the case of a monochromatic pump. For a fluctuating pump, we have to specify the nature of the pump, i. e., we have to specify the stochastic processes $\mu(t)$ and $\mathcal{E}_0(t)$. The model, for which exact solutions could be obtained, corresponds to (i) $\mathcal{E}_0(t)$ being a time-independent constant, and (ii) $\mu(t)$ being a Gaussian delta correlated process, i. e.,

$$\langle \mu(t)\mu(t') \rangle = 2\gamma_c \delta(t-t'), \quad \langle \mu(t) \rangle = 0. \quad (2.19a)$$

This is the familiar phase-diffusion model of the laser light in which the amplitude remains constant. In this model the amplitude correlations are given by

$$\langle \mathcal{E}^*(t)\mathcal{E}(t') \rangle = \exp\{-\gamma_c |t-t'|\}, \quad \langle \mathcal{E}(t)\mathcal{E}(t') \rangle = 0 \quad (2.19b)$$

i. e., the spectrum is Lorentzian. Higher-order correlations of the field have more complicated structure, though these can be evaluated in a closed form.²⁵ The method of calculation for the above model is similar to that given in Ref. 21. Let us denote the ensemble-averaged values of $\tilde{\rho}_{ij}$ over the distribution of $\mu(t)$ by $\Psi_{ij} = \langle \tilde{\rho}_{ij} \rangle$. Using the general theory of Ref. 21, we then find the equations of motion for Ψ_{ij} :

$$\begin{aligned} \dot{\Psi}_{++} &= i\alpha(\Psi_{g+} - \Psi_{+g}) - 2\gamma\Psi_{++}, \\ \dot{\Psi}_{--} &= i\alpha(\Psi_{g-} - \Psi_{-g}) - 2\gamma\Psi_{--}, \\ \dot{\Psi}_{gg} &= i\alpha(\Psi_{+g} + \Psi_{-g} - \Psi_{g+} - \Psi_{g-}) + 2\gamma(\Psi_{++} + \Psi_{--}), \\ \dot{\Psi}_{+-} &= i\alpha(\Psi_{g-} - \Psi_{+g}) - (2\gamma + i\delta)\Psi_{+-}, \\ \dot{\Psi}_{+g} &= i\alpha(\Psi_{gg} - \Psi_{+-} - \Psi_{-+}) - (2i\delta + \gamma + \gamma_c)\Psi_{+g}, \\ \dot{\Psi}_{-g} &= i\alpha(\Psi_{gg} - \Psi_{+-} - \Psi_{-+}) - (i\delta + \gamma + \gamma_c)\Psi_{-g}. \end{aligned} \quad (2.20)$$

The above equations no longer involve any explicit time dependence and could be solved in a straightforward manner. The solutions of these equations can then be used to obtain the detection signals. The fluorescence signals detected along

y and x directions, denoted respectively by L_y and L_x , with polarizations along x and y , respectively, are given by [cf. Ref. 10]

$$\begin{aligned} L_x &\propto \rho_{++} + \rho_{--} + 2\text{Re}\rho_{+-}, \\ L_y &\propto \rho_{++} + \rho_{--} - 2\text{Re}\rho_{+-}. \end{aligned} \quad (2.21)$$

Substituting for the density matrix elements ρ_{ij} 's in terms of $\bar{\rho}_{ij}$'s we obtain

$$L_x \propto \bar{\rho}_{++} + \bar{\rho}_{--} - 2(\text{Re}\bar{\rho}_{+-}\cos 2\theta + \text{Im}\bar{\rho}_{+-}\sin 2\theta), \quad (2.22)$$

$$L_y \propto \bar{\rho}_{++} + \bar{\rho}_{--} + 2(\text{Re}\bar{\rho}_{+-}\cos 2\theta + \text{Im}\bar{\rho}_{+-}\sin 2\theta),$$

and hence the ensemble-averaged signals will be

$$\begin{aligned} \langle L_x \rangle &\propto \Psi_{++} + \Psi_{--} - 2(\text{Re}\Psi_{+-}\cos 2\theta + \text{Im}\Psi_{+-}\sin 2\theta), \\ \langle L_y \rangle &\propto \Psi_{++} + \Psi_{--} + 2(\text{Re}\Psi_{+-}\cos 2\theta + \text{Im}\Psi_{+-}\sin 2\theta). \end{aligned} \quad (2.23)$$

In the following section, the set of equations (2.20) is solved analytically under steady-state conditions and the analytical expressions for the fluorescence signals are obtained. The signals are studied as a function of δ for various values of the parameters, such as field strengths and bandwidths. Hereafter, the ensemble-averaged signals will be denoted by L_x and L_y , with the angular brackets omitted for simplicity.

III. ANALYTICAL AND NUMERICAL RESULTS FOR THE FLUORESCENCE SIGNALS

The fluorescence signals L_x and L_y defined in the previous section are determined by the steady-state solutions of the density matrix elements Ψ_{++} , Ψ_{--} , and Ψ_{+-} . Under steady-state conditions, the left-hand side of the set of equations (2.20) becomes zero. Therefore, these nine algebraic equations can be solved analytically. A long but straightforward calculation yields the results

$$\Psi_{++} + \Psi_{--} = 2\alpha^2\mu[(4\gamma^2\mu^2 + 4\alpha^2\mu + \delta^2)(\delta^2\mu + 4\gamma^2\mu + 4\alpha^2) + 9\delta^2(\delta^2 + 4\gamma^2)\mu]D^{-1}, \quad (3.1)$$

which for $\delta \rightarrow 0$ goes over to $2\alpha^2/(4\alpha^2 + \gamma^2\mu)$, which in the limit of strong and weak fields further reduces to

$$\Psi_{++} + \Psi_{--} = \begin{cases} \frac{1}{2} & \text{for } \alpha^2 \gg \gamma^2\mu, \quad \delta = 0 \\ 2\alpha^2/\gamma^2\mu & \text{for } \alpha^2 \ll \gamma^2\mu, \quad \delta = 0. \end{cases} \quad (3.2)$$

In Eq. (3.1), μ and D are given by

$$\mu = 1 + (\gamma_c/\gamma),$$

$$\begin{aligned} D = & \left(\gamma^2\mu^2 + 4\alpha^2\mu + 2\delta^2 + \frac{\delta^2\alpha^2(1-\mu)}{(4\gamma^2 + \delta^2)} \right) [(4\gamma^2\mu^2 + 4\alpha^2\mu + \delta^2)(4\gamma^2\mu + \delta^2\mu + 4\alpha^2) + 9\delta^2(\delta^2 + 4\gamma^2)\mu] \\ & + (\delta^2/2) \left(9\delta^2 + (4\gamma^2\mu^2 + 4\alpha^2\mu + \delta^2) \frac{(4\alpha^2 - 4\gamma^2 - \delta^2)}{(4\gamma^2 + \delta^2)} \right) [2\alpha^2(\mu - 1) - \mu(4\gamma^2 + \delta^2)]. \end{aligned} \quad (3.3)$$

The atomic coherences are given by

$$\text{Re}\Psi_{+-} = \alpha^2\mu[(\delta^2 + 4\gamma^2\mu^2 + 4\alpha^2\mu)(4\gamma^2\mu + 4\alpha^2 - \delta^2) + 9\delta^2(\delta^2 + 4\gamma^2)\mu]D^{-1}, \quad (3.4)$$

which for $\delta \rightarrow 0$ goes over to $\alpha^2/(4\alpha^2 + \gamma^2\mu)$, which in the limiting cases further reduces to

$$\text{Re}\Psi_{+-} = \begin{cases} \frac{1}{4} & \text{for } \alpha^2 \gg \gamma^2\mu, \\ \alpha^2/\gamma^2\mu & \text{for } \alpha^2 \ll \gamma^2\mu, \end{cases} \quad \delta = 0. \quad (3.5)$$

Similarly we have the results

$$\text{Im}\Psi_{+-} = 2\alpha^2\mu\delta\gamma[9\delta^2(1-\mu) - (4\gamma^2\mu^2 + 4\alpha^2\mu + \delta^2)(1+\mu)]D^{-1}, \quad (3.6)$$

$$\text{Im}\Psi_{--} \rightarrow 0 \text{ as } \delta \rightarrow 0. \quad (3.7)$$

Now, let us examine the symmetry properties of the above expressions when we change δ to $-\delta$. We see that $(\Psi_{++} + \Psi_{--})$ and $\text{Re}\Psi_{+-}$ are even functions of δ , and $\text{Im}\Psi_{+-}$ is an odd function of δ . The symmetry properties of the fluorescence signals depend on the direction of polarization of the incident pump field. We note that

$$\begin{aligned} L_x(-\delta) &= L_x(\delta), \\ L_y(-\delta) &= L_y(\delta), \end{aligned} \quad (3.8)$$

for $\theta = 0, \pi/2$ etc., i. e., $L_x(\delta)$ and $L_y(\delta)$ are symmetric about $\delta = 0$ for these values of θ . Moreover, for $\theta = \pi/4, \frac{3}{4}\pi$ etc. we have the relations

$$\begin{aligned} L_x(\delta) &= L_y(-\delta), \\ L_y(\delta) &= L_x(-\delta). \end{aligned} \quad (3.9)$$

Let us now consider some special cases under which the expressions for signals have a simplified form.

A. Monochromatic pump

Let us first examine the results for the case of narrow-band excitation, i. e., in the limit $\gamma_c \rightarrow 0$, for an arbitrary strength of the linearly polarized pump laser. In this limit, the results are given by

$$(\Psi_{++} + \Psi_{--}) = 2\alpha^2 [9\delta^2(\delta^2 + 4\gamma^2) + (4\gamma^2 + \delta^2 + 4\alpha^2)^2] D_1^{-1}, \quad (3.10)$$

$$\text{Re}\Psi_{+-} = \alpha^2 [(\delta^2 + 4\gamma^2 + 4\alpha^2)(4\gamma^2 + 4\alpha^2 - \delta^2) + 9\delta^2(\delta^2 + 4\gamma^2)] D_1^{-1}, \quad (3.11)$$

and

$$\text{Im}\Psi_{+-} = -4\gamma\delta\alpha^2(4\gamma^2 + 4\alpha^2 + \delta^2) D_1^{-1}, \quad (3.12)$$

where

$$D_1 = (\gamma^2 + 4\alpha^2 + \frac{3}{2}\delta^2)[9\delta^2(\delta^2 + 4\gamma^2) + (\delta^2 + 4\gamma^2 + 4\alpha^2)^2] + \delta^2[(4\gamma^2 + 4\alpha^2 + \delta^2)(\delta^2 + 4\gamma^2)]. \quad (3.13)$$

The positions and widths of peaks in $(\Psi_{++} + \Psi_{--})$, etc., could be ascertained from the roots of D_1 , which are rather complicated as D_1 is cubic in δ^2 .

Now, if we assume, as usual, that the pump is weak, i. e., $\alpha \ll \gamma$, then in this limit the results of (3.10) to (3.13) simplify considerably to

$$(\Psi_{++} + \Psi_{--}) = \alpha^2 \left(\frac{1}{\delta^2 + \gamma^2} + \frac{1}{4\delta^2 + \gamma^2} \right), \quad (3.14)$$

$$\text{Re}\Psi_{+-} = \frac{\alpha^2}{3} \left(\frac{1}{\delta^2 + \gamma^2} + \frac{2}{4\delta^2 + \gamma^2} \right), \quad (3.15)$$

and

$$\text{Im}\Psi_{+-} = \frac{2}{3} \alpha^2 \frac{\delta}{\gamma} \left(\frac{1}{\delta^2 + \gamma^2} - \frac{4}{4\delta^2 + \gamma^2} \right). \quad (3.16)$$

B. Broadband pump

As Hanle experiments have been performed with both monochromatic and broadband sources, it is worthwhile to examine the effect of the source bandwidth on the nature of the spectra. We first consider the weak field spectra $\alpha \ll \gamma, \gamma_c$. In this case, expressions (3.1) to (3.6) simplify to

$$(\Psi_{++} + \Psi_{--}) = \alpha^2 \mu \left(\frac{1}{(4\delta^2 + \gamma^2 \mu^2)} + \frac{1}{(\delta^2 + \gamma^2 \mu^2)} \right), \quad (3.17)$$

$$\text{Re}\Psi_{+-} = \frac{2\alpha^2}{(\delta^2 + 4\gamma^2)} \left(\frac{(\mu + 2)}{(\mu^2 - 16)} + \frac{(\mu - 1)}{(\mu^2 - 4)} \right) - \frac{2\mu\alpha^2(\mu^2 - 16)^{-1}(\mu + 4)}{(4\delta^2 + \gamma^2 \mu^2)} + \frac{\mu(\mu^2 - 4)^{-1}\alpha^2(\mu - 2)}{(\delta^2 + \gamma^2 \mu^2)}, \quad (3.18)$$

$$\text{Im}\Psi_{+-} = \frac{\delta}{\gamma} \alpha^2 \left(\frac{[(2 - \mu)(\mu^2 - 4)^{-1} - (\mu + 1)(\mu^2 - 16)^{-1}]}{(\delta^2 + 4\gamma^2)} + \frac{4(1 + \mu)(\mu^2 - 16)^{-1}}{(4\delta^2 + \gamma^2 \mu^2)} - \frac{(2 - \mu)(\mu^2 - 4)^{-1}}{(\delta^2 + \gamma^2 \mu^2)} \right). \quad (3.19)$$

We can see from the above that the fluorescence signal for $\theta = 0, \pi/2$ etc. is a sum of three Lorentzians, with the possibility of the weight factors associated with some of them being negative, of widths 2γ , $\gamma\mu$, and $\gamma\mu/2$, respectively. For the case $\theta = \pi/4$, the signal has, in addition to the above, a dispersive contribution which comes from the term $\text{Im}\Psi_{+-}$. Although the signal has a dispersive contribution, it always remains positive. For

In this limit, it can be seen that each of the functions $(\Psi_{++} + \Psi_{--})$ and $\text{Re}\Psi_{+-}$ can be expressed as the sum of two Lorentzians, one with a width γ and the other with a width $\gamma/2$. $\text{Im}\Psi_{+-}$ is dispersive in nature, which results from its dependence on δ . Therefore, the signal for the case $\theta = 0, \pi/2$ etc. could be written as the sum of two Lorentzians (the weight factor associated with one of them may be negative) of widths γ and $\gamma/2$, respectively, and for the case when $\theta = \pi/4, 3\pi/4$ there are two dispersion terms in the signal which come from the term $\text{Im}\Psi_{+-}$, in addition to the absorption type of terms. The results (3.14) to (3.16) are in agreement with a recent work of Delsart *et al.*¹⁷

arbitrary values of the strength of the broadband field, the signals are examined in the next section.

From the analytical expressions given above, it is difficult to get an insight into the actual behavior of the fluorescence signals $L_x(\delta)$ and $L_y(\delta)$. Therefore, we now proceed to present some of the numerical results for the line shapes of the fluorescence signals $L_x(\delta)$ and $L_y(\delta)$, for various values of the field strengths and the fluctuation parameter

γ_c , as functions of δ .

The normalized plot of the signal $L_x(\delta)$, i. e., of $L_x(\delta)/L_x(0)$, which is detected along the x direction with its polarization vector directed along the y direction, as a function of δ , for $\theta = \pi/2$, for the weak-field case is shown in Fig. 3. This signal is a symmetric function of δ . It can be seen that with increase in γ_c , the line broadens. It is to be noted that the value $\delta = 0$ corresponds to the zero value of the intensity of the circularly polarized light. Figure 4 shows the normalized plot (normalized so that the maximum value is unity) of the signal $L_y(\delta)$, detected along the y direction with its polarization parallel to the x direction, for $\theta = \pi/2$, for the weak-field case. The signal $L_y(\delta)$, which is symmetric with respect to δ , has a double-humped structure. Here, again, a similar effect, as in the case of Fig. 3 viz. broadening of the line with increase in γ_c , is observed. In both the above cases (Figs. 3 and 4) it is seen that the lines are much narrower with monochromatic excitation ($\gamma_c = 0$) than with broadband excitation. A similar result was found by Rasmussen *et al.*⁵ for the case of usual magnetic-field Hanle effect.

Figure 5 is a plot of the fluorescence signal $L_x(\delta)$ for the weak-field case for $\theta = \pi/4$. It is to be noted that the signal for $\theta = \pi/4$ has the property $L_x(\delta) = L_y(-\delta)$, and vice versa. The signal has a single-peaked structure with slight asymmetry about $\delta = 0$. As the fluctuations become larger, the asymmetry increases and the line attains a dispersive shape for large enough γ_c . However, the signal always remains positive. Here, the signal for the case when $\gamma_c = 10$ has been magnified by a factor of 10.

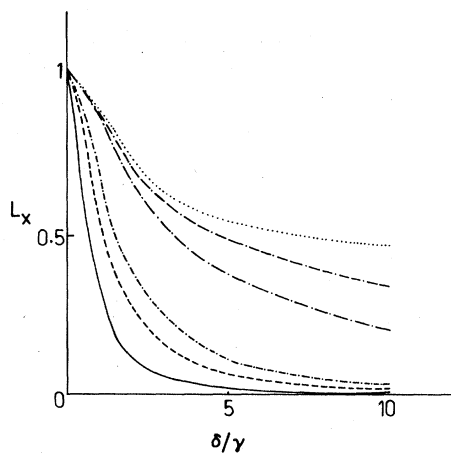


FIG. 3. The normalized fluorescence signal L_x as a function of δ for $\theta = \pi/2$, $\alpha = .01$, $\gamma = 1$, and for the following values of the bandwidth parameter γ_c : (a) $\gamma_c = 0$; (b) $\gamma_c = 1$; (c) $\gamma_c = 2$; (d) $\gamma_c = 10$; (e) $\gamma_c = 20$; (f) $\gamma_c = 50$.

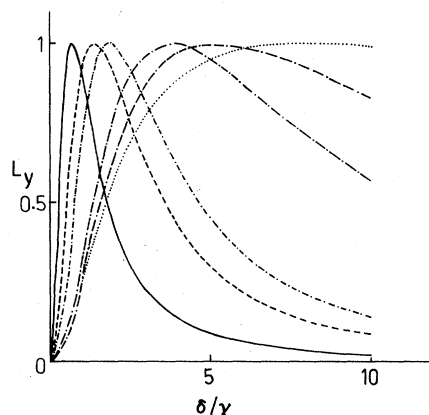


FIG. 4. The normalized fluorescence signal L_y as a function of δ for the same values of parameters as in Fig. 3.

Figure 6 shows the normalized fluorescence signal $L_x(\delta)$, for $\theta = \pi/2$, for the strong-field case. The signal has a similar shape to that of the weak-field case, but with a much larger magnitude than that of the weak-field case, which is due to saturation effects [cf. Eq. (3.2)]. In Fig. 7, the normalized fluorescence signal $L_y(\delta)$ for the case when $\theta = \pi/2$ is plotted for the strong-field case. Here, again, the signal has a double-humped structure like that of the weak-field case. The width of the signal (i. e., dip at the origin) does not depend critically on the width of the pump laser, in contrast to the weak-field case. The width first increases slightly with increase in γ_c and then decreases with further increase in γ_c . One may compare the results of

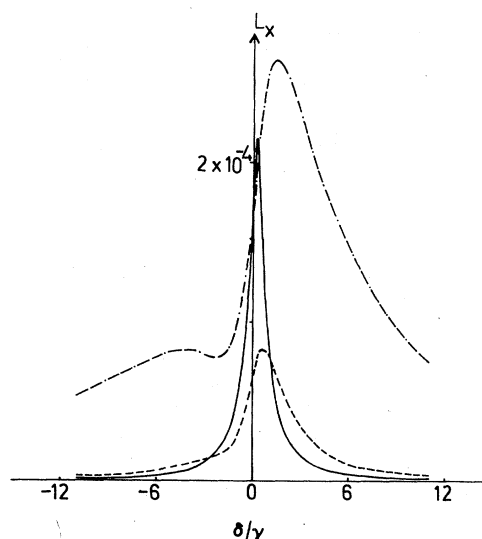


FIG. 5. The fluorescence signal L_x as a function of δ for $\theta = \pi/4$, $\alpha = 0.01$, $\gamma = 1$, and for the following values γ_c : (a) $\gamma_c = 0$; (b) $\gamma_c = 2$; (c) $\gamma_c = 10$.

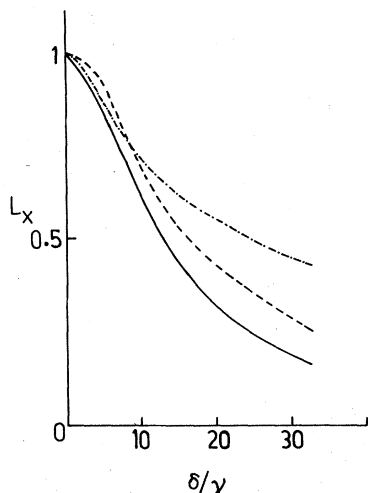


Fig. 6. The normalized fluorescence signal L_x as a function of δ for $\theta = \pi/2$, $\alpha = 10$, $\gamma = 1$, and for the following values of γ_c : (a) — $\gamma_c = 0$; (b) - - - $\gamma_c = 2$; (c) - · - · $\gamma_c = 10$.

Figs. 6 and 7 with those of Avan and Cohen Tannoudji¹⁰ for the case of the usual magnetic-field Hanle effect. We see that the qualitative effect of bandwidth on the optical Hanle signals is similar to that in the case of magnetic-field Hanle effect. We also note that the optical Hanle signals do not show very pronounced narrowing due to laser line-width, as is typical of the magnetic-field Hanle effect. The differences may be due to the fact that the pumping laser is always asymmetrically off the two atomic transitions, due to Stark shifts induced by the nonresonant laser.²⁶

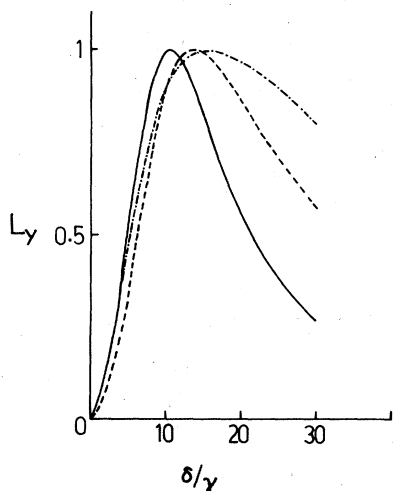


FIG. 7. The normalized fluorescence signal L_y as a function of δ for the same values of parameters as in Fig. 6.

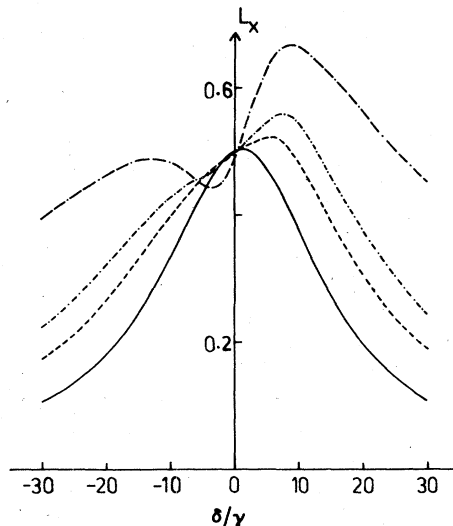


FIG. 8. The fluorescence signal L_x as a function of δ for $\theta = \pi/4$, $\alpha = 10$, $\gamma = 1$, and for values of the bandwidth parameter γ_c as: (a) — $\gamma_c = 0$; (b) - - - $\gamma_c = 1$; (c) - · - · $\gamma_c = 2$; (d) · · · $\gamma_c = 10$.

In Fig. 8, a plot of the fluorescence signal $L_x(\delta)$, for $\theta = \pi/4$, for the strong-field case is shown. For the narrow-band excitation, the line has a single peaked structure with slight asymmetry about $\delta = 0$. As the fluctuations are increased, the asymmetry becomes more pronounced and the line attains a dispersive shape. However, it is to be noted that the signal always remains positive.

IV. OPTICAL HANLE EFFECT UNDER STRONG BROADBAND EXCITATION

In this section, we outline an alternate approach to the Hanle effect in strong broadband fields, although in the literature several treatments¹¹ of the broadband fields already exist. We will use some general results from the theory of multiplicative stochastic processes. We assume that the broadband field could be represented by a delta correlated Gaussian random process. Both these assumptions are justified in view of the central-limit theorem, since a broadband field, in principle, can be represented by a superposition of an infinitely large number of modes. Therefore, the electric field $\vec{\mathcal{E}}(t)$ in (2.13) is now regarded as a Gaussian stochastic process with correlation function

$$\langle \mathcal{E}'(t) \mathcal{E}'^*(t') \rangle = 2D\delta(t-t'), \quad \langle \mathcal{E}'(t) \mathcal{E}'(t') \rangle = 0 \quad (4.1)$$

where

$$\vec{\mathcal{E}}(t) = \mathcal{E}'(t)(\hat{x} \cos\theta + \hat{y} \sin\theta). \quad (4.2)$$

On using (2.15) and (4.2), the Hamiltonian $H'(t)$ simplifies to

$$H'(t) = \hbar(\omega_0 - \omega_L + \delta)A_{++} + \hbar(\omega_0 - \omega_L - \delta)A_{gg} + [A_{+g}g'(t)^{-i\theta} - A_{-g}g'(t)^{i\theta} + \text{H. c.}]. \quad (4.3)$$

On using the theory of multiplicative stochastic processes,²⁷ the ensemble average of $\rho^{(R)}$ can be written as

$$\begin{aligned} \frac{\partial}{\partial t} \langle \rho^{(R)} \rangle &= L_{\text{inc}} \langle \rho^{(R)} \rangle - i[(\omega_0 - \omega_L + \delta)A_{++} + (\omega_0 - \omega_L - \delta)A_{gg}, \langle \rho^{(R)} \rangle] \\ &\quad - (R^2/\hbar^2)D[A_{+g}e^{-i\theta} - A_{-g}e^{i\theta}, [A_{+g}e^{i\theta} - A_{-g}e^{-i\theta}, \langle \rho^{(R)} \rangle]] \\ &\quad - (R^2/\hbar^2)D[A_{+g}e^{i\theta} - A_{-g}e^{-i\theta}, [A_{+g}e^{-i\theta} - A_{-g}e^{i\theta}, \langle \rho^{(R)} \rangle]]. \end{aligned} \quad (4.4)$$

On making use of the transformation of type (2.16) (with φ replaced by zero), the equations of motion for the ensemble-averaged elements of the density matrix are now given by

$$\begin{aligned} \dot{\Psi}_{++} &= -2(\gamma_1 + \gamma)\Psi_{++} - D_0(2\Psi_{++} + \Psi_{+-} + \Psi_{-+} - 2\Psi_{gg}), \\ \dot{\Psi}_{--} &= -2(\gamma_1 + \gamma)\Psi_{--} - D_0(2\Psi_{--} + \Psi_{+-} + \Psi_{-+} - 2\Psi_{gg}), \\ \dot{\Psi}_{gg} &= p - 2\gamma_0\Psi_{gg} + 2\gamma(\Psi_{++} + \Psi_{--}) + 2D_0(\Psi_{++} + \Psi_{--} + \Psi_{+-} + \Psi_{-+} - 2\Psi_{gg}), \\ \dot{\Psi}_{+-} &= -(2\gamma + 2\gamma_1 + i\delta)\Psi_{+-} - D_0(2\Psi_{+-} + \Psi_{++} + \Psi_{--} - 2\Psi_{gg}), \\ \dot{\Psi}_{+g} &= -(\gamma_0 + \gamma_1 + \gamma + 2i\delta)\Psi_{+g} - D_0(\Psi_{+g} + 3\Psi_{-g}), \\ \dot{\Psi}_{-g} &= -(\gamma_0 + \gamma_1 + \gamma + i\delta)\Psi_{-g} - D_0(\Psi_{-g} + 3\Psi_{+g}), \end{aligned} \quad (4.5)$$

where $R^2D/\hbar^2 = D_0$ and where we have also included the incoherent decay of the levels $J=0$ and $J=1$ at the rates $2\gamma_0$ and $2\gamma_1$, respectively, as well as the pumping of the level $J=0$ at the rate p . This kind of situation was considered by Carrington and Corney and Ducloy,¹¹ who also assumed that $\gamma \ll \gamma_0$ and γ_1 , in the context of the usual Hanle effect. The steady-state solutions of Eqs. (4.5) are given by

$$(\Psi_{++} + \Psi_{--}) = \frac{D_0 p}{\Lambda} \left(1 - \frac{4D_0\gamma_0(\gamma_1 + \gamma)(\gamma_1 + \gamma + D_0)}{(\delta^2 + \Gamma^2)\Lambda} \right), \quad (4.6)$$

$$\text{Re}\Psi_{+-} = \frac{2D_0 p (\gamma + \gamma_1)^2 [1 + D_0/(\gamma + \gamma_1)]}{(\delta^2 + \Gamma^2)\Lambda}, \quad (4.7)$$

$$\text{Im}\Psi_{+-} = \frac{-\delta D_0 p (\gamma_1 + \gamma)}{(\delta^2 + \Gamma^2)\Lambda}, \quad (4.8)$$

where

$$\Gamma^2 = \frac{4[(\gamma + \gamma_1 + 2D_0)\gamma_0 + 2D_0\gamma_1](\gamma + \gamma_1 + D_0)(\gamma + \gamma_1)}{\Lambda} \quad (4.9a)$$

and

$$\Lambda = [(\gamma_1 + \gamma + D_0)\gamma_0 + 2D_0\gamma_1]. \quad (4.9b)$$

The fluorescence signals L_x and L_y for the case when $\theta = \pi/2$ are given by

$$L_x(\theta = \pi/2) = \frac{D_0 p}{\Lambda} \left(1 + \frac{4(\gamma + \gamma_1)^2 [1 + D_0/(\gamma + \gamma_1)] [(\gamma + \gamma_1)\gamma_0 + 2D_0\gamma_1]}{(\delta^2 + \Gamma^2)\Lambda} \right), \quad (4.10)$$

$$L_y(\theta = \pi/2) = \frac{D_0 p}{\Lambda} \left(1 - \frac{4(\gamma + \gamma_1)^2 [1 + D_0/(\gamma + \gamma_1)] [(\gamma + \gamma_1)\gamma_0 + 2D_0(\gamma_0 + \gamma_1)]}{(\delta^2 + \Gamma^2)\Lambda} \right). \quad (4.11)$$

The above results, which are valid to all powers in D_0 and for arbitrary values of decay parameters γ_0 , γ_1 , and γ , have been derived rigorously under the assumption of a delta correlated Gaussian pump field. Ducloy, in an extensive study²⁸ of the magnetic-field Hanle effect, has examined the nature of the Hanle signals in the presence of a broadband field. He considered the broadband field to be a superposition of a large number of laser modes, with the spacing between the laser

modes taken to be much smaller than say the width of the excited state. His model of the broadband laser is very much like our model (4.1). It is interesting to note that our results for optical Hanle signals in broadband fields are rather similar to those for the magnetic-field Hanle signals—the most important property being the Lorentzian characteristic of the signals, with intensity-dependent detunings.

The degree of polarization produced by the pump

radiation for the case when $\theta = \pi/2$ is given by

$$P\left(\theta = \frac{\pi}{2}\right) = \frac{|L_x - L_y|}{L_x + L_y} = \frac{2 \operatorname{Re}\Psi_{+-}}{\Psi_{++} + \Psi_{--}} = \frac{\Gamma_0^2}{\Gamma_0^2 + \delta^2}, \quad (4.12)$$

where the full width at half-maximum of the degree of polarization signal is given by

$$\Gamma_0 = 2(\gamma + \gamma_1)[1 + D_0/(\gamma + \gamma_1)]^{1/2}. \quad (4.13)$$

It is important to note that the width of the polarization as a function of δ , for the case when $\theta = \pi/2$, does not depend on the decay rate γ_0 of the ground state, although the width of the signals L_x and L_y does depend on the parameter γ_0 .

A series expansion of (4.6), (4.7), and (4.8) in powers of the intensity parameter D_0 leads to

$$\begin{aligned} (\Psi_{++} + \Psi_{--}) &= \frac{pD_0}{\gamma_0(\gamma_1 + \gamma)} \\ &\quad - \frac{D_0^2 p}{\gamma_0^2} \left(\frac{\gamma_0}{X} + \frac{(\gamma_0 + 2\gamma_1)}{(\gamma + \gamma_1)^2} \right) + \dots, \end{aligned} \quad (4.14)$$

$$\begin{aligned} \operatorname{Re}\Psi_{+-} &= \frac{2p(\gamma + \gamma_1)D_0}{\gamma_0 X} \\ &\quad - \frac{4p[\gamma_1 X + 4\gamma_0(\gamma + \gamma_1)^2]D_0^2}{\gamma_0^2 X^2} + \dots, \end{aligned} \quad (4.15)$$

$$\begin{aligned} \operatorname{Im}\Psi_{+-} &= \frac{-\delta p D_0}{\gamma_0 X} \\ &\quad + \left(\frac{(2\gamma_1 + \gamma_0)}{\gamma_0^2(\gamma + \gamma_1)} + \frac{8(\gamma + \gamma_1)}{\gamma_0 X} \right) \frac{\delta p D_0^2}{X} + \dots, \end{aligned} \quad (4.16)$$

where

$$X = [\delta^2 + 4(\gamma + \gamma_1)^2]. \quad (4.17)$$

The results of (4.14) to (4.16) in the limit when $\gamma \ll \gamma_0$ and γ_1 are in agreement with the general observations and remarks made by Ducloy¹¹ in the context of the usual magnetic-field Hanle effect studies. Recently, Delsart *et al.*²⁹ have reported the experimental results on optical Hanle signals both in monochromatic as well as in broadband fields. They consider the case in which the saturation effects are not important. The experimental observations, say in the broadband case, can be explained in terms of the first term in the series expansions like (4.15) and (4.16).

ACKNOWLEDGMENT

One of us (P.A.L.) would like to thank the Council of Scientific and Industrial Research, New Delhi for the award of Junior Research Fellowship.

¹B. Decomps, M. Dumont, and M. Ducloy, in *Laser Spectroscopy*, edited by H. Walther (Springer, New York, 1976), Vol. 2, p. 283.

²H. Walther, in *Laser Spectroscopy*, edited by H. Walther (Springer, New York, 1976), Vol. 2, p. 1.

³C. G. Carrington and A. Corney, *Opt. Commun.* **1**, 115 (1969); *J. Phys. B* **4**, 849 (1971).

⁴I. Colomb, M. Gorlicki, and M. Dumont, *Opt. Commun.* **21**, 289 (1977); M. Gorlicki and M. Dumont, *ibid.* **11**, 166 (1974).

⁵W. Rasmussen, R. Schieder, and H. Walther, *Opt. Commun.* **12**, 315 (1974).

⁶D. Lecler, R. Ostermann, W. Lange, and J. Luther, *J. Phys. (Paris)* **36**, 647 (1975).

⁷S. J. Silvers and M. R. McKeever, *Chem. Phys.* **27**, 27 (1978).

⁸A. Corney, in *Atomic and Laser Spectroscopy* (Oxford University Press, Oxford, 1977), p. 473.

⁹R. C. Hilborn and R. L. de Zafra, Jr., *Opt. Soc. Am.* **62**, 1492 (1972).

¹⁰P. Avan and C. Cohen Tannoudji, *J. Phys. B* **10**, 171 (1977).

¹¹C. G. Carrington and A. Corney, *Opt. Commun.* **7**, 30 (1973); M. Ducloy, *ibid.* **8**, 17 (1973).

¹²J. N. Dodd and G. W. Series, *Proc. R. Soc. London* **263**, 353 (1961).

¹³A. Corney and G. W. Series, *Proc. Phys. Soc. London* **83**, 207 (1964); **83**, 213 (1964).

¹⁴B. P. Kibble and G. W. Series, *Proc. Phys. Soc. London* **78**, 70 (1961).

¹⁵V. P. Kaftandjian and L. Klein, *Phys. Lett.* **A62**, 317 (1977).

¹⁶V. P. Kaftandjian, L. Klein, and W. Hanle, *Phys. Lett.* **A65**, 188 (1978).

¹⁷C. Delsart, J. C. Keller, and V. P. Kaftandjian, *Proceedings of the Fourth International Conference on Laser Spectroscopy*, 1979, edited by H. Walther and K. W. Rotho (Springer, New York, 1979), p. 618.

¹⁸V. S. Letokhov and V. P. Chebotayev, in *Nonlinear Laser Spectroscopy* (Springer, New York, 1977), Sec. 4, Vol. 4, p. 169.

¹⁹J. E. Bjorkholm and P. F. Liao, in *Laser Spectroscopy*, edited by S. Haroche *et al.* (Springer, New York, 1975), Vol. 43, p. 176.

²⁰S. Reynaud, M. Himbert, J. Dupong-Roc, A. H. Stroke, and C. Cohen Tannoudji, *Phys. Rev. Lett.* **42**, 756 (1979).

²¹G. S. Agarwal, *Phys. Rev. A* **18**, 1490 (1978), and the references cited therein.

²²G. S. Agarwal, in *Springer Tracts in Modern Physics*, edited by G. Höhler *et al.* (Springer, New York, 1974), Sec. 6, Vol. 70.

²³N. N. Bogoliubov and J. A. Mitropolsky, in *Asymptotic Methods in the Theory of Nonlinear Oscillations* (Hindustan, Delhi, 1961), Chap. 5.

²⁴Reference 22, Appendix A.

²⁵G. S. Agarwal, *Phys. Rev. A* **1**, 1445 (1970).

²⁶It would perhaps be interesting to study the optical Hanle signals with the pump laser off the resonance frequency corresponding to the $J=0$ to $J=1$ transition.

The magnetic-field Hanle signals in this situation for zero bandwidth of the field have been reported by P. Avan and C. Cohen Tannoudji, *J. Phys. Lett. (Paris)* 36, L85 (1975).

²⁷Reference 21, Appendix B.

²⁸M. Ducloy, *Phys. Rev. A* 8, 1844 (1973); *A* 9, 1319 (1973).

²⁹C. Delsart, J. C. Keller, and V. P. Kaftandjian, *Opt. Commun.* 32, 406 (1980).